

TESLA LINEAR COLLIDER DESIGN AND R&D STATUS

R. Brinkmann (for the TESLA Collaboration)
DESY, D-22603 Hamburg, Germany

Abstract

This paper summarises the present status of the overall design and of the technical developments for a next generation e+e- linear collider based on superconducting linac technology.

1 INTRODUCTION

Studies towards a next generation e+e- Linear Collider in the 0.5 - 1 TeV centre-of-mass energy range are being pursued world-wide by several High Energy Physics laboratories. In the international TESLA collaboration, centred at DESY, more than 30 institutes from Armenia, China, Finland, France, Germany, Italy, Poland, Russia and USA participate in the design work and technical R&D for a linear collider based on superconducting Niobium accelerating structures (Fig. 1) operated at 2K. The combination of high AC-to-beam power transfer efficiency $\eta_{AC \rightarrow b}$ with small emittance dilution in the low-frequency (1.3 GHz) linac makes this choice of technology ideally suited for an optimum performance in terms of the achievable luminosity and operation stability.

A considerable challenge results from the need to reduce the cost per unit accelerating voltage by a large factor compared to existing large-scale installations of superconducting cavities (e.g. at LEP and CEBAF). Our aim is to increase the accelerating gradient by about a factor of five to ~ 25 MV/m and simultaneously reduce the cost per unit length by a factor of four.

In the following, the progress on the design of the TESLA Linear Collider facility and the status of the R&D programme at the TESLA Test Facility (TTF) will be summarised.



Fig. 1: The 9-cell TESLA Niobium cavity

2 OVERALL LAYOUT AND PARAMETERS

The layout of TESLA is sketched in Fig. 2. The total site length is about 33 km, including the beam delivery system (which provides beam collimation and spot size demagnification). A complete description of the machine, including all sub-systems such as cryogenic plants, damping rings, particle sources, etc. is given in the design report published in spring 1997 [1]. The report includes chapters on the Particle Physics and the layout of the Detector, which were prepared in a joint study of DESY and ECFA. The integration of an X-ray coherent light source user facility into the TESLA project is also part of the 1997 design study.

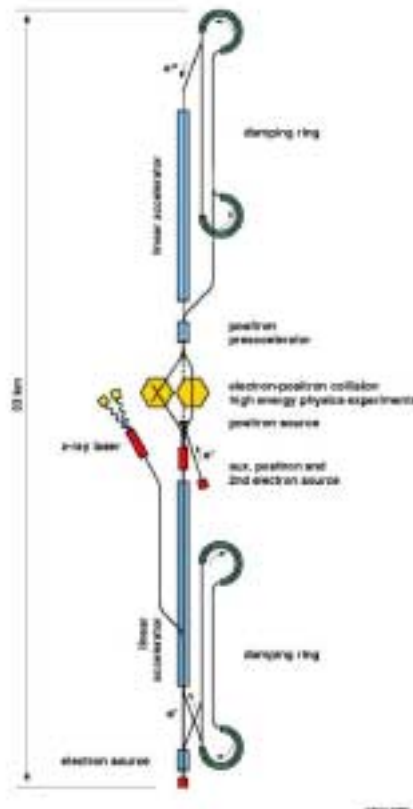


Fig.2: Overall layout of TESLA

During the past years we have performed a re-optimisation of the machine sub-systems with the primary goal of exploiting the full performance potential of

TESLA. The main machine parameters at a centre-of-mass energy of $E_{cm} = 500$ GeV are shown in Table 1. In comparison with the original parameters [1], the design luminosity has been increased by almost a factor of five. The modifications of the individual sub-systems of the collider, in particular in view of the improved parameter set, are described in more detail in Sections 3-6.

The progress on superconducting cavity R&D (Section 7) indicates that the accelerating gradient can be pushed beyond the value of 22MV/m required for $E_{cm} = 500$ GeV. The sub-systems of the facility (in particular the beam delivery system) have been laid out such as to accommodate an energy upgrade to $E_{cm} = 800$ GeV. The gradient required for this energy within the given site length for the 500 GeV facility is 35 MV/m, well below the theoretical limit for the Niobium resonators (>50 MV/m). The machine parameters at 800 GeV, which assume an upgrade of the cryogenic plants and of the RF-system (doubling the number of klystrons) are shown in Table 1.

Table 1: TESLA parameters at $E_{cm} = 500$ and 800 GeV.

	500 GeV	800 GeV
site length [km]	32.8	32.8
active length [km]	23	23
acc. Gradient [MV/m]	22	35
quality factor Q_n [10^{10}]	1	0.5
t_{pulse} [μ s]	950	860
# bunches n_b /pulse	2820	4526
bunch spacing Δt_b [ns]	337	190
rep. rate f_{rep} [Hz]	5	4
N_b /bunch [10^{10}]	2	1.4
ϵ_x / ϵ_y at IP [10^{-6} m]	10 / 0.03	8 / 0.015
beta at IP β_{xy}^* [mm]	15 / 0.4	15 / 0.4
spot size σ_x^* / σ_y^* [nm]	553 / 5	391 / 2.8
bunch length σ_z [mm]	0.3	0.3
beamstrahlung δ_R [%]	3.3	4.7
Disruption D_v	25	28
P_{AC} (2 linacs) [MW]	100	160
efficiency $\eta_{AC \rightarrow b}$ [%]	23	20
lumin. L [10^{34} cm $^{-2}$ s $^{-1}$]	3.4	4.3

3 MAIN LINAC

The layout of the linear accelerator described in [1] assumed an arrangement with groups of 8 9-cell superconducting resonators per cryogenic module very similar to the ones built for the TTF. One drawback of this scheme is a rather low filling factor ($\eta_{fill} =$ ratio of active length to total length), partly due to the large spacing of 1.5 wavelengths between resonators. New schemes with reduced spacing between cavities have been worked out [2], which improve η_{fill} from 66% to 76...80%. The most

economic solution is the “superstructure” concept where several multi-cell cavities are grouped together with one-half wavelength in between and the RF-power fed in from one side by a single input coupler. This also strongly reduces the number of input couplers and simplifies the rf-distribution system. For $\eta_{fill} = 76\%$ and an unchanged total site length, the required gradient at $E_{cm} = 500$ GeV goes down to 22 MV/m. This leads to a reduction of power for the cryogenic plants which can be invested into rf-power and to an improvement of beam pulse to rf-pulse length due to a lower loaded quality factor Q_{ext} . As a result, the overall power transfer efficiency goes up from originally 17% to 23%. The required power for each of the 300 klystrons per linac is 8.2 MW, still leaving a regulation and safety margin of 20% w.r.t. the design power of 10 MW per klystron. A multi-beam, high efficiency klystron has been developed in industry. Tests with a first prototype showed an RF-power of 10MW at 1.5ms pulse length according to design and an efficiency of 65%, compared to the design value of 70%.

Beam dynamics in the main linac, which were shown to be very uncritical in the reference design, become more of an issue with the beam emittance reduced by an order of magnitude. Tracking simulations have been performed assuming transverse alignment tolerances of 500 μ m for the cavities and 10 μ m for the BPM’s relative to quadrupole axis (obtained by beam-based alignment). The resulting vertical emittance growth amounts to 10...20% from both single-bunch and multi-bunch effects. Especially for the latter case, this can not be simply interpreted as incoherent spot size dilution when determining the impact on the luminosity. Rather, the centroids of the bunches in a train are at different positions in phase space at the end of the linac with the result of vertical offsets at the IP. Since these offsets are critical (see section 6), a further reduction of multi-bunch effects is desirable. Fortunately, most of the multi-bunch effect is “static” (i.e. reproducible from pulse to pulse), because it results from HOM excitation in the displaced cavities and a slow variation of bunch energy over the length of the pulse from Lorentz-force detuning (most, but not all of which is removed by the rf-feedback system). We therefore expect that the multi-bunch emittance dilution can be strongly reduced with the help of fast kickers, which are present in any case as part of the foreseen fast (i.e. bunch-to-bunch) orbit feedback system. This has recently been studied [3] by simulating the time evolution of the multi-bunch orbit pattern at the end of the linac under the influence of diffusive ATL-like ground motion. It turns out that the random motion of quadrupoles causes almost exactly only a drift in the *average* orbit, while the individual bunch positions w.r.t. to the average change only by a tiny fraction: for an average drift of a few μ m (about one vertical sigma) the rms-variation of the multi-bunch orbit pattern is only of the order of a few nm. We conclude that much of the

effect of HOM is static and can be very efficiently removed by the feedback system.

4 DAMPING RING

The damping ring design represents a compromise between a reasonable upper limit for the circumference and a lower limit for the injection/extraction system bandwidth. The “dogbone” design chosen here accommodates 90% of the 17 km long ring in the linac tunnel, thus saving considerable civil construction cost. The beam-optical design of the ring has recently been improved [4], driven by concerns regarding the incoherent space charge tune shift ΔQ_{inc} which can become large due to the unconventional ratio of ring circumference to beam energy. As a first measure to reduce ΔQ_{inc} the energy was raised from 3.2 to 5 GeV, accompanied by an optimisation of the arc lattice to maintain the required small horizontal emittance. As a second step we introduce a closed betatron coupling bump in the straight sections of the ring which strongly increases the beam cross section by making it “round” and reduces the space charge force by almost an order of magnitude. Computer simulations including space charge have been performed [4] and it could be shown that the detrimental effect of incoherent tune spread, which can cause emittance growth by resonance crossing, was almost completely removed.

While a damping ring will certainly be required for the positron beam which has initially a very large transverse and longitudinal emittance, it is conceivable to generate an electron beam of sufficiently good quality directly from a low-emittance photocathode RF-gun. We have developed a new scheme [5,6] which combines a low-emittance gun similar to those used for Free Electron Lasers with a special beam optics adapter to transform the naturally round beam from the gun into a flat one ($\epsilon_x \gg \epsilon_y$) suitable for the Linear Collider. According to computer simulations [6], this concept has the potential to eliminate the electron damping ring and thus reduce the cost and complexity of the collider facility. A successful first experimental proof of this new concept was recently done at the FNAL A0 experiment [7].

5 POSITRON SOURCE

The TESLA positron source is based on the concept of high-energy photon conversion into e^+e^- pairs in a thin target [8]. The photons are generated by the high-energy electron beam which is sent through a wiggler. Advantages of this concept are a low heat load on the target and a higher capture efficiency for the e^+ beam behind the target. In our original layout [1] it was foreseen to use the electron beam after the IP to drive the positron source. However, the spent beam exhibits a large energy spread due to beamstrahlung which makes chromatic correction difficult and collimation of the low-energy tail necessary. The technical and radiation safety problems

resulting from the need to collimate about 10% (~1MW average beam power) of the spent beam led us to move the positron source to a position upstream from the IP (directly after the e- linac) and use the incoming beam to produce the photons. Besides avoiding the collimation problem, this layout has the advantage of facilitating the generation of polarised positrons, since the emittance requirements for that option, where the wiggler is replaced by a helical undulator, are easily met by the incoming electron beam. The disadvantages of this modified set-up are a few hundred meters of additional tunnel length, an increase in the beam energy spread from 0.5×10^{-3} to 1.8×10^{-3} (the beam emittance is only slightly affected by the synchrotron radiation emitted in the wiggler/undulator) and an additional low-energy transfer line to transport the positrons after pre-acceleration [9] to the other side of the interaction region.

6 DELIVERY SYSTEM AND BEAM-BEAM EFFECTS

The 1.6km long beam line between the end of the linac and the IP [10] comprises of a collimation section to remove small amounts of beam halo, which could otherwise cause background at the experiment, and of a Final Focus section responsible for de-magnifying the beam size to the small dimensions required at the IP.

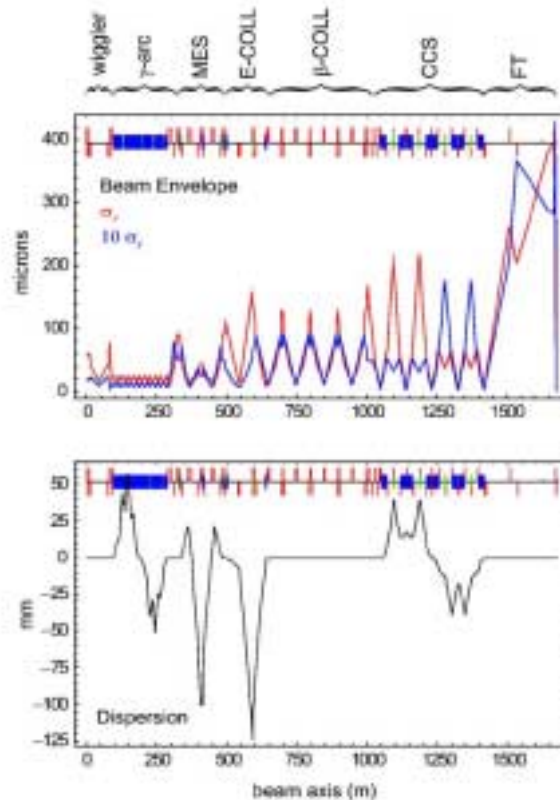


Fig. 3: Beam optics of the delivery system

The present layout has separate sections for energy and betatron collimation. In the dispersive energy collimation

section a non-linear insertion is used which provides an increase of the beam cross section at the position of the downstream collimator in case of an energy error outside the delivery system acceptance ($\sim 2\%$). Such beam energy offsets can be caused during a linac pulse by RF-system failures and are supposed to be much more likely than large transverse orbit offsets due to magnet failures. With the increased beam size, the collimator can stand the loss of several bunches in the train, which gives sufficient time to trigger an emergency extraction kicker to direct the rest of the beam pulse towards the main beam dump.

The transverse collimation section consists of a periodic lattice of cells with 45 deg. phase advance in between the collimator positions. The collimator aperture of $1.5\text{mm}\times 0.5\text{mm}$ corresponds to $12\sigma_x\times 80\sigma_y$. The beta functions in this section are sufficiently high to allow for an accurate measurement of the beam size using wire systems.

The TESLA e+e- interaction region is laid out for head-on collision, separation of the beams takes place after the superconducting final doublet by means of an electrostatic deflector. The modification of the positron source concept (Section 5) led us to re-optimize the spent beam extraction scheme [11]. The main beams as well as the beamstrahlung are passed almost loss-free to absorbers 250m downstream from the IP.

The large disruption parameter makes the luminosity very sensitive to relative offsets of the colliding beams in vertical position or angle at the IP. We designed a fast orbit feedback system [12] which, thanks to the large spacing between bunches, can operate on a bunch-to-bunch basis and maintains head-on collision accurate to one tenth of a standard deviation in orbit and angle. This safely limits the reduction in luminosity to less than 10% even in an environment with relatively large ground vibration amplitudes, such as observed in the interaction regions of the HERA ring [13].

In contrast to bunch centroid offsets, which can be very efficiently removed by the feedback, internal bunch deformations ("banana" shape from short-range wakefields) represent a somewhat more subtle problem. Such deformations are amplified during collision due to the large disruption, which can give rise to a luminosity reduction larger than naively estimated from the projected emittance growth. This issue is presently being investigated in detail.

The delivery system layout includes a beam switch yard [9] in order to be able to serve a second interaction region. Switching beams between the two IR's could take place either on a pulse-to-pulse basis or on a longer time scale. The geometry of the second beamline is such as to yield a 30mrad crossing angle at the IP. This is necessary if the 2nd IR is to be used for a $\gamma\gamma$ -collider option (see e.g. Appendix A in ref. [1] for an overview of the $\gamma\gamma$ -option). Using the 2nd IP for e+e- collisions is not excluded, though, and since beam separation happens after the

wiggler producing photons for the positron source, construction of a 2nd e+ source will not be necessary.

7 TEST FACILITY (TTF)

The s.c. cavity development program was launched by the TESLA collaboration in 1992 [14]. The test facility built at DESY includes clean rooms for preparation and assembly, chemical treatment, ultra-pure high-pressure water rinsing and heat treatment of Nb cavities. Single cavities undergo tests with cw-RF excitation in a vertical cryostat and in pulsed mode on a horizontal test stand ("CHECHIA"), before they are installed in a cryo-module which houses 8 9-cell cavities. A summary of cavity performance on the vertical test stand is given in Fig. 4.

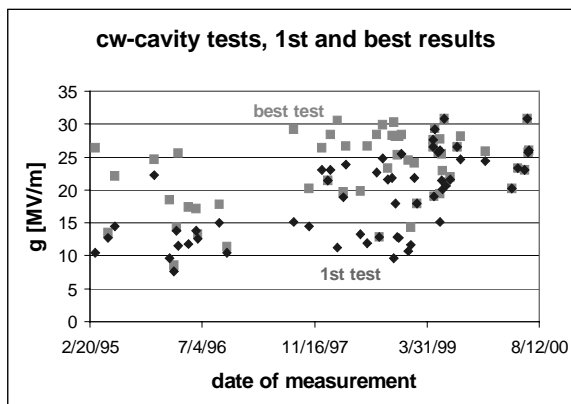


Fig. 4: Cavity performance on the vertical test stand

Here, a distinction is made between results of the first test, after a resonator has once passed through the standard procedure, and the best result after applying additional processing. The performance improvement over the past years is clearly visible. In particular, the reliability with which good cavities are produced has steadily been improved. Fig. 5 shows the rate of success defined as the percentage of cavities reaching more than 20MV/m in first cw-test. The TESLA500 goal of 22MV/m at $Q_0 = 10^{10}$ is reached by these cavities *on average*.

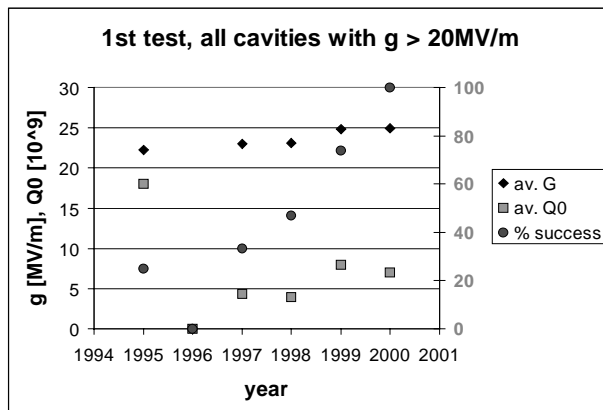


Fig. 5: Rate of success for cavities with $g > 20\text{MV/m}$ and average gradient and Q_0 for this sub-set of cavities

The ongoing R&D program [15,16] focuses on possible simplifications in the cavity production and treatment and on pushing the performance towards higher gradients. Recent developments in electropolishing, which are done in collaboration between CERN, KEK, Saclay and DESY, have yielded very high accelerating gradients (35...40 MV/m with Q_0 close to 10^{10}) in several single cell resonators. It is particularly remarkable that this performance was achieved without high-temperature (1400 C) treatment, instead a bake-out at very moderate (~130 C) temperature was applied. Once this method can be established for multicell-cavities, there is potential not only for achieving the gradient required for the TESLA energy upgrade, but simultaneously simplifying the treatment procedure.

One potential problem arising at high gradient is the detuning from resonance during the RF-pulse due to the Lorentz force. It was recently demonstrated that the detuning can be actively compensated by means of a piezo element integrated in the mechanical tuning device [15], so that we will not need additional regulation RF-power for operation at higher gradient.

Two methods for fabrication of cavities without welding seams are experimentally studied: spinning [17] and hydroforming [18]. One of the hydroformed resonators, after electropolishing showed a record value for the gradient in a single cell cavity (Fig. 6).

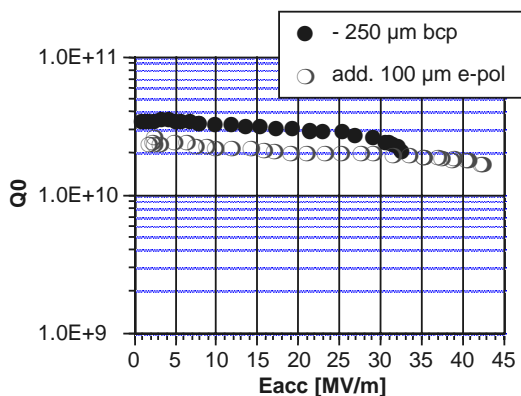


Fig. 6: Performance of a single cell hydroformed cavity before and after electropolishing [17]

A full integrated system test with beam is done at the TTF linac. The linac went into operation in May 1997 and up to date three accelerator modules have been tested (the 3rd one replaced module #1). The measured average gradient was 16MV/m, 20.5MV/m and 22MV/m, for modules #1, 2 and 3, respectively. During the past year a major fraction of beam time was dedicated to the commissioning and studies of the SASE Free Electron Laser concept. First lasing at about 100nm wavelength was achieved in Feb. 2000. For a summary of the FEL operation experience, see refs. [19,20].

8 CONCLUSIONS

The TESLA collaboration has worked out a complete design for a high-performance next generation Linear Collider at 500-800 GeV based on superconducting linac technology. The achievements at the Test Facility demonstrate the availability of the technology for 500 GeV energy. The R&D programme towards higher gradients is continuing and the recent progress justifies the optimism that the required higher gradient for 800 GeV is in reach.

DESY as the co-ordinating institute of the collaboration has taken over the task to do the preparations necessary to make a site for the TESLA facility available in the North-West region of Germany, next to the DESY site. The central area, 16.5km from the DESY site, will accommodate both the High Energy Physics experiments and the Free Electron Laser user facility.

The collaboration is presently preparing a Technical Design Report, which will include estimates of project cost, construction schedule and required work force and which is scheduled to be published in spring 2001.

REFERENCES

- [1] R. Brinkmann, G. Materlik, J. Roßbach and A. Wagner (eds.), DESY-1997-048.
- [2] M. Liepe and J. Sekutowicz, contribution to this conference.
- [3] N. Baboi, to be published.
- [4] W. Decking and R. Brinkmann, contribution to EPAC, Vienna 2000.
- [5] R. Brinkmann, Y. Derbenev and K. Flöttmann, DESY-TESLA-99-09.
- [6] R. Brinkmann, Y. Derbenev and K. Flöttmann, contribution to EPAC, Vienna 2000.
- [7] D. Edwards et al., contribution to this conference.
- [8] V. E. Balakin and A. A. Mikhailichenko, Preprint INP-79-85, Novosibirsk 1979.
- [9] V. V. Balandin, N. I. Golubeva, L. V. Kravchuk, V. A. Moiseev, V. V. Paramonov and K. Flöttmann, contribution to EPAC, Vienna 2000.
- [10] R. Brinkmann, N. Walker, O. Napoly and J. Payet, contribution to EPAC, Vienna 2000.
- [11] E. Merker, I. Yazynin, O. Napoly, R. Brinkmann, N. Walker and A. Drozhdin, contribution to EPAC, Vienna 2000.
- [12] I. Reyzl, contribution to EPAC, Vienna 2000.
- [13] C. Montag, contribution to EPAC, Vienna 2000.
- [14] D. Edwards (ed.), DESY-TESLA-93-01.
- [15] M. Liepe, contribution to this conference.
- [16] D. Trines, contribution to EPAC, Vienna 2000.
- [17] P. Kneisel and V. Palmieri, Proc. PAC, New York 1999, p. 943.
- [18] W. Singer, I. Gonin, I. Jelezov, H. Kaiser, T. Khabibuline, P. Kneisel, K. Saito and X. Singer, contribution to EPAC, Vienna 2000.
- [19] J. Roßbach, contribution to EPAC, Vienna 2000.
- [20] P. Castro-Garcia, contribution to this conference.